Integrative and Comparative Biology
Integrative and Comparative Biology, pp. 1–13
doi:10.1093/icb/icy121
Society for Integrative and Comparative Biology

SYMPOSIUM ARTICLE

Body Flexibility Enhances Maneuverability in the World's Largest Predator

P. S. Segre,[1,*] D. E. Cade,[*] J. Calambokidis,[†] F. E. Fish,[‡] A. S. Friedlaender,[§] J. Potvin[¶] and J. A. Goldbogen[*]

*Hopkins Marine Station of Stanford University, 120 Ocean View Blvd, Pacific Grove, CA 93950, United States; †Cascadia Research Collective, 218 1/2 4th Avenue W, Olympia, WA 98501, USA; ‡West Chester University, 750 South Church Street, West Chester, PA 19383, USA; §University of California, Santa Cruz, 1156 High Street, Santa Cruz, CA 95064, USA; ¶Saint Louis University, Saint Louis, MO 63103, USA

[1]E-mail: psegre@stanford.edu

Synopsis Blue whales are often characterized as highly stable, open-ocean swimmers who sacrifice maneuverability for long-distance cruising performance. However, recent studies have revealed that blue whales actually exhibit surprisingly complex underwater behaviors, yet little is known about the performance and control of these maneuvers. Here, we use multi-sensor biologgers equipped with cameras to quantify the locomotor dynamics and the movement of the control surfaces used by foraging blue whales. Our results revealed that simple maneuvers (rolls, turns, and pitch changes) are performed using distinct combinations of control and power provided by the flippers, the flukes, and bending of the body, while complex trajectories are structured by combining sequences of simple maneuvers. Furthermore, blue whales improve their turning performance by using complex banked turns to take advantage of their substantial dorso-ventral flexibility. These results illustrate the important role body flexibility plays in enhancing control and performance of maneuvers, even in the largest of animals. The use of the body to supplement the performance of the hydrodynamically active surfaces may represent a new mechanism in the control of aquatic locomotion.

Introduction

Animals in motion face the conflicting demands of stability and maneuverability while performing a wide range of critical life functions such as foraging and long-distance migration (Fish 2002). The same morphologies that create stability also make the asymmetrical force generation that initiates and maintains maneuvers more difficult to execute. Through the varied location, morphology, and use of control surfaces animals may prioritize stability or maneuverability (Weihs 1993; Fish 2004). In swimming animals, control and propulsion surfaces can either generate destabilizing forces to initiate maneuvers or provide dynamic stabilization by coordinating their phased oscillation with different body parts (Fish et al. 2003b; Weber et al. 2014; Fish and Lauder 2017). At large scales, swimming animals use wing-shaped control surfaces to generate hydrodynamic lift, which is used to power locomotion and perform maneuvers (Webb 1988; Fish and Battle 1995; Fish 1996; Sfakiotakis et al. 1999; Fish and Lauder 2017). Because lift is proportional to the surface area of the control surfaces while resistance to acceleration is dependent on body volume, the isometric scaling of area and volume suggests that larger animals will suffer decreased maneuverability (Webb and De Buffrénil 1990). However, this scaling relationship should also cause larger animals to be highly stable and resistant to perturbations, which decreases the cost of steady state rectilinear locomotion and together with lower mass-specific metabolic rate should favor life-history traits like trans-oceanic excursions and foraging in pelagic habitats (Williams 1999; Fish 2002).

As expected, many large whale species travel long distances across extensive home ranges that span across ocean basins. As a result of this observation and the tradeoff between maneuverability and stability (Fish 2002; Webb 2004), the foraging capacity of large whale species has been characterized as slow, lacking agility, and generally likened to a "grazing" strategy that consists of maintaining low feeding costs while exploiting large amounts of low quality food (Williams 2006). Although some large whale species like bowhead whales forage at low speeds (Simon et al. 2009), many of the largest filter feeding rorqual species (Balaenopteridae) and raptorial sperm whales target prey with well developed escape responses that require high speed attacks and complex trajectories (Aoki et al. 2012; Cade et al. 2016). These studies suggest that agility in the largest cetaceans is crucial to efficiently capture smaller, more maneuverable prey; but, precisely how large whales use their control surfaces to execute these maneuvers is not known.

A central feature of cetacean locomotion is the separation of propulsion and control: dorso-ventral fluke strokes generate power, while direction and stability are controlled with anteriorly located flippers (Fish 2004). However, recent studies have also documented situations where the flippers are used for propulsion (Segre et al. 2017) and the flukes are used to help execute maneuvers (Fish 2002), illustrating the fact that little is known about how these large animals control their movements. Nevertheless, cetacean flippers are thought to be the primary control surface responsible for performing longitudinal axis rolls (spinner dolphins: Fish et al. 2006; fin whales: Segre et al. 2016), turns (humpback whales: Edel and Winn 1978), and pitch changes (minke whales: Cooper et al. 2008). Although the primary role of cetacean flukes is to power locomotion, small toothed whales can twist their flukes to an upright position and use them as a rudder, particularly when they are not fluking (Fish 2002). There is also mixed evidence on whether twisting the flukes can assist the flippers for performing rolls (spinner dolphins: Fish et al. 2006; fin whales: Segre et al. 2016). The role of such body flexion in effecting cetacean maneuvers is poorly understood but it should enhance turning ability relative to a rigid body (Fish 2004). Dorsal flexibility may facilitate upward and downward direction changes, whereas lateral flexibility may influence turning radius (Long et al. 1997; Fish 2002). Taken together, a general picture on how cetaceans use their control surfaces to maneuver emerges, but these concepts remain poorly tested, particularly in natural environments. Furthermore, most of our collective knowledge comes from smaller dolphins in captivity, whereas very little is known about how maneuvers are performed by the largest cetaceans, which have very different sizes, morphologies, and ecological niches that likely require different locomotor strategies and foraging mechanisms. Here we provide a unique investigation into the mechanisms of control and agility at the largest scale, by directly quantifying the maneuvers of free-swimming blue whales (*Balaenoptera musculus*). Specifically, we use a newly developed multi-sensor tag with integrated cameras to identify stereotyped maneuvers; quantify their performance; and determine how the movement of the flippers, flukes, and body are used to initiate and maintain simple and complex maneuvers. Given their enormous size, we expect blue whales will have limited body flexibility along the dorsal, ventral, and torsional axes and therefore will rely on their flippers to effect direction changes along the roll, pitch, and yaw axes.

Materials and methods

Data collection

Between 2014 and 2017 we deployed suction-cup attached, multi-sensor biologging tags on 16 individual Northeast Pacific blue whales in CA, USA. The whales were approached in a small boat and the tags were temporarily attached using a 6-m long carbon-fiber pole. Once the suction cups detached from the whale, the tags floated to the surface and were localized and recovered using radio telemetry. The tags (Customized Animal Tracking Solutions; Goldbogen et al. 2017) were equipped with three-axis accelerometers (400 Hz), magnetometers (50 Hz), gyroscopes (50 Hz), pressure, and temperature sensors (10 Hz), and one or two video cameras with a variety of capabilities (Cade et al. 2016). After the tags were recovered the accelerometer and magnetometer data were aligned with the body axis of the whale and then smoothed with a low pass filter (two-pass Butterworth, cutoff frequency =0.08 Hz) to obtain the orientation of the body while removing most of the fluctuations caused by the fluke strokes. These data were then used to calculate the pitch, roll, and heading of the whale (Johnson and Tyack 2003). A non-dimensional representation of the fluke strokes was created by calculating pitch from the unsmoothed sensor data and then filtering with a bandpass filter (two-pass Butterworth, cutoff frequencies 0.4 and 0.08 Hz) to remove sampling error and the effects of changes in body orientation (Sato et al. 2007). Translational speed was determined by calibrating measurements of the background accelerometer vibrations with the orientation-corrected depth rate for each tag orientation, on each individual (Cade et al. 2018).

Data analysis

Using the processed data we identified simple pitching, rolling, and turning maneuvers that were performed along a single axis of motion. We defined pitching maneuvers as segments where the pitch velocity started and ended at zero and the absolute value of the pitch change was more than 45°. Furthermore we only used pitching maneuvers where the maximum roll was less than 30° from upright and the change in roll was less than 30°. For each pitching maneuver, we calculated the maximum angular velocity along the pitch axis. We defined rolls as maneuvers where the roll velocity started and ended at zero and the change in roll was more than 45°. We only used rolls where the maximum pitch angle was between −30° and 30° from horizontal and the pitch change was less than 30°, and where the heading change was less than 30°. For each rolling maneuver we calculated the maximum roll angle, and the maximum angular velocity of the roll. We defined turns as maneuvers where the heading change velocity started and ended at zero and the heading change was more than 45°. We only used turns where the maximum pitch angle was between −30° and 30° from horizontal and the pitch change was less than 30°, but we did not constrain roll. For each turn we calculated the maximum roll angle and the maximum angular velocity of the heading change. We only used maneuvers that occurred while the cameras were recording. Data analysis was performed using Matlab (Mathworks) and Python (Python Software Foundation).

To determine the roles that the flippers, flukes, and body flexion play on the initiation and maintenance of the maneuvers, we compared still images taken from the videos at the start, at the time of the maximum angular velocity (midpoint), and at the end of the maneuver. The precise orientation of the cameras varied with each deployment and not every control surface was visible in every frame. Because of the limitations of using a single camera view we used a subjective scoring system to determine the position of the control surfaces. We scored the position of the flippers as extended (highly protracted and elevated) or not-extended. We also scored the rotation of the flippers between the start and midpoint of the maneuver (rotated up, rotated down). We scored the position of the body in the coronal plane as dorsally-extended or not-extended (which included neutral and ventrally flexed positions) and in the sagittal plane as laterally flexed or neutral. To determine torsion along the longitudinal axis, we scored the orientation of the flukes relative to the rolling direction (neutral, lowered leading, or trailing side). For pitching maneuvers, we scored the position of the flippers at the midpoint of the maneuver, the rotation of the flippers at the start and the midpoint, and the dorsal extension at the midpoint. For rolls, we scored the position of the flippers at the start and the midpoint of the maneuvers, the rotation of the flippers between the start and the midpoint, and the torsion of the flukes at the midpoint. For turns we scored the position of the flippers and the dorsal and lateral extension of the body at the midpoint of the turn. Using the non-dimensional representation of the fluke strokes we categorized each maneuver as powered or unpowered.

Statistical analysis

Our approach to understanding the biomechanical control of blue whale maneuvering performance is inherently limited by the capabilities and placement of the cameras. Therefore, to avoid over-interpreting our data we limit our analysis of the photographic data to descriptive statistics. We present the number of observations where a characteristic occurs out of the total number of observations. The total number of observations only includes maneuvers where the characteristic is observable and unambiguous, therefore the total number of observations is often less than the total amount of maneuvers recorded. To compare performance between different types of maneuvers we use a linear mixed effects model with individual as a random effect. Numerical data are presented as mean plus one standard deviation of the mean. Statistical significance was determined as $P < 0.05$. Statistics were performed in Python using the Statsmodels package.

Results

Flipper excursion and body flexibility

Blue whale flippers move along three axes (Fig. 1A): protracting and retracting along the cranial–caudal axis of the body, elevating and depressing along the dorso-ventral axis, and rotating about their longitudinal axis so that the leading edge is oriented upward or downward relative to the direction of travel. In a fully protracted and elevated position the flippers form a right angle with the body (Fig. 1B, C), and the flippers can rotate upward or downward. From this position the flippers can be depressed approximately 90° so that they are directly underneath the body (Fig. 1D). In this position it is unknown how much the flippers can rotate. In a fully retracted position the flipper is aligned with the long axis of the whale and rotated so that it sits flush against the lateral aspect of the body

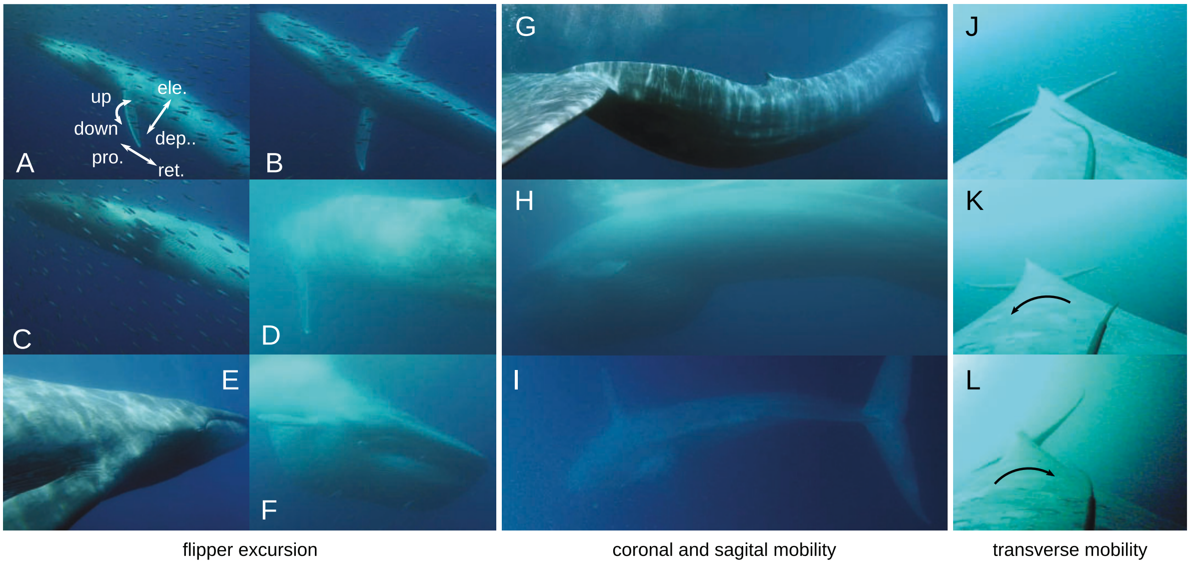

Fig. 1 The range of motion of blue whale flippers, body axis, and fluke torsion as documented by external and whale-born cameras. **A**) Flippers can be elevated and depressed along the dorso-ventral axis, protracted and retracted along the cranio-caudal axis, and rotated about the longitudinal axis so that the leading edge is oriented upward or downward. **B**) A whale with elevated, protracted flippers near the limits of their excursion. The flipper rotations are asymmetric. **C**) A lateral view of the elevated and protracted left flipper with an upward rotation. **D**) The left flipper in a fully depressed and protracted orientation. **E**) The right flipper is fully retracted. **F**) During filtering the right flipper is elevated and semi-protracted. **G**) The body is dorsally extended with the flippers in a protracted and depressed position as the whale surfaces. **H**) The body is ventrally flexed immediately after leaving the surface with a mouthful of water. **I**) A dorsal view of left lateral flexion. **J**) A dorsally oriented, whale-deployed camera shows the flukes in a neutral position while the whale is not maneuvering. **K**) The same camera shows the torsion of the flukes during a rightward roll. The trailing edge is lowered. **L**) The camera records the lowered trailing edge of the flukes during a roll to the left. Images A–I courtesy of the BBC.

(Fig. 1E). During filtering the buccal pouch expands and may constrain the flipper position so that it cannot fully retract or depress (Fig. 1F). Given their body size and weight, blue whales demonstrate a notable amount of body flexibility in the coronal, sagittal, and transverse planes. In the coronal plane, blue whales have a high degree of extension (Fig. 1G) and flexion (Fig. 1H), both of which are used to power the fluke strokes. Blue whales also demonstrate a substantial amount of lateral flexion from the midsagittal plane (Fig. 1I). Finally, blue whales have limited torsion in the transverse plane. In spite of the length of the body and the flukes, we never observed the flukes to be twisted more than approximately 45° from the neutral position (Fig. 1J, K, L).

Pitch changes

We recorded 415 pitch changes from 14 whales, 359 downward and 56 upward (Fig. 2 and Table 1). Downward pitch changes had faster angular velocities than upward pitch changes (mean of means ±SD; down: 5.8°/s ± 1.6; up: 5.0°/s±1.3; $P = 0.002$). Downward pitch changes were characterized by flippers that were not in a fully elevated and protracted position during the middle of the maneuver (159/173; not elevated-protracted/total observations), a downward flipper rotation (37/39), and a neutral or flexed dorsal body position (278/282). Powered downward pitch changes ($n = 343$) were significantly faster than unpowered ($n = 16$) downward pitch changes (powered: −6.4°/s±1.1; unpowered: −2.2°/s±0.4; $P < 0.001$). Upward pitch changes were characterized by flippers that were in a fully elevated and protracted position during the middle of the maneuver (19/20), an upward flipper rotation (20/20), and an extended dorsal body position (21/23). Powered upward pitch changes ($n = 49$) were significantly faster than unpowered ($n = 7$) upward pitch changes (powered: 5.1°/s±1.4; unpowered: 3.8°/s±0.6; $P = 0.04$).

Rolls

We recorded 181 rolls from 12 whales, 110 were used for maneuvering, and 71 occurred during the filtering that takes place after lunge feeding events (Fig 3; Table1). Maneuvering rolls had faster maximum roll velocities than filtering rolls (mean of means ±SD; maneuvering: 9.4°/s±3.0; filtering: 6.9°/s±2.1; $P < 0.001$). Maneuvering rolls were characterized by flippers that mostly started in an elevated, protracted position (46/69), but the flippers only sometimes stayed in an elevated-protracted position throughout the fastest point of the roll (36/68), although there was a lot of variability. Between the start and the midpoint of the maneuvering roll, the leading flipper rotated downward and the trailing flipper rotated upward (53/53). Filtering rolls were characterized by flippers that started in an elevated, protracted position (32/35) and the flippers mostly stayed in an elevated, protracted position throughout the fastest point in the roll (20/36). Between the start and the midpoint of the filtering roll, the leading flipper rotated downward and the trailing flipper rotated upward (26/27). The fluke rotation was only visible in four rolls (all were maneuvering rolls) and in all cases the side of the fluke opposite to the direction of the roll was lower than the neutral position (4/4). Powered maneuvering rolls ($n=89$) were significantly faster than unpowered ($n=21$) maneuvering rolls (powered: 10.2°/s±2.4; unpowered: 5.5°/s±1.9; $P=0.03$), but the rolling velocity of powered filtering rolls ($n=23$) was not significantly different than the velocity of unpowered ($n=48$) filtering rolls (powered: 6.9°/s±3.1; unpowered: 6.0°/s±1.6; $P=0.85$).

Turns

We recorded 356 turns from 16 whales, 143 were level turns (<10° roll), 205 were banked inward and 8 were banked outward (Fig. 4; Table 1), although the outward banked turns were only rolled slightly more than 10° (mean of means ±SD: 12.6° ±1.8). Inward banked turns had higher angular velocities than level turns (inward: 5.8°/s±2.3; level: 2.7°/s±0.8; $P<0.001$). Of the inward banked turns only 3 were performed at the surface (3/205), in contrast with the level turns where 120 were performed at the surface (120/143). Inward banked turns were characterized by elevated and protracted flippers (101/115) and a dorsally extended body (88/121) at the midpoint of the turn. Some of the inward banked turns were performed with a body flexed laterally in the direction of the turn (46/79). Level turns were characterized by flippers that were not in an elevated-protracted position (65/73) and a dorsally neutral body (108/111) at the midpoint of the turn. Many of the level turns were performed with a body flexed laterally in the direction of the turn (29/42). Powered turns ($n=314$) were not significantly faster than unpowered ($n=42$) turns (powered: 4.0°/s±1.2; unpowered: 3.7°/s±1.1; $P=0.22$).

Discussion

Blue whale flipper excursion and body flexibility: comparisons to other cetaceans

Blue whales have highly mobile flippers. Their range of motion along the elevation–depression axis is similar to that of humpback whales (Edel and Winn 1978; Woodward 2006; Fish et al. 2011). Blue whales apparently can retract their flippers to a greater extent than many other cetaceans, but not as much as sperm whales and beaked whales; however, humpback whales can protract their flippers to a much greater degree than blue whales (Segre et al. 2017). Although we do not have robust data on the limits of flipper rotation about the longitudinal axis, it appears that blue whales cannot rotate their flippers to the same extant as humpback whales (Edel and Winn 1978). Blue whales also demonstrate a notable amount of body flexibility, in spite of their extreme body size. Furthermore, it appears that both dorsal and lateral flexibility play an important role in performing angular changes of direction. Although other cetaceans may be able to use fluke torsion to perform rolls (Fish et al. 2006), we have only observed a limited amount of possible fluke torsion in blue whales, and we have not observed fluke-driven rolling.

The role of flippers, flukes, and body flexibility in the performance of maneuvers

Blue whales perform pitching maneuvers using their coronal plane flexibility: to pitch upward they dorsally extend their back (Figs. 2A, D and 5B) and to pitch downward they ventrally flex their body (Figs. 2B, E and 5A). Upward pitch changes often feature elevated and protracted flippers rotated upward, a position that generates maximum, symmetrical, upward hydrodynamic lift (Fig. 2A, D). However during downward pitch changes the flippers are often not in an elevated and protracted position (Fig. 2B, E), which suggests that they are not as important to performing the downward maneuver. Perhaps their negative body density allows blue whales to perform downward pitch changes by flexing and reorienting their body. Many rapid pitch changes occur near the surface (Fig. 2C, E) as the whale rises toward the sea surface to breathe. These maneuvers are associated with substantial flipper movement, both positional and rotational, but the flippers are almost always kept underwater as the whale surfaces (Fig. 2C, E).

Feeding blue whales make extensive use of longitudinal axis body rolls to scout and approach their prey (Goldbogen et al. 2012; Friedlaender et al. 2017). Rolls are performed by generating asymmetric hydrodynamic forces with the flippers (Figs. 3A-C and 5C, D). To begin the roll, both flippers are elevated and protracted and the outside flipper rotates upward generating upward lift, while the inside

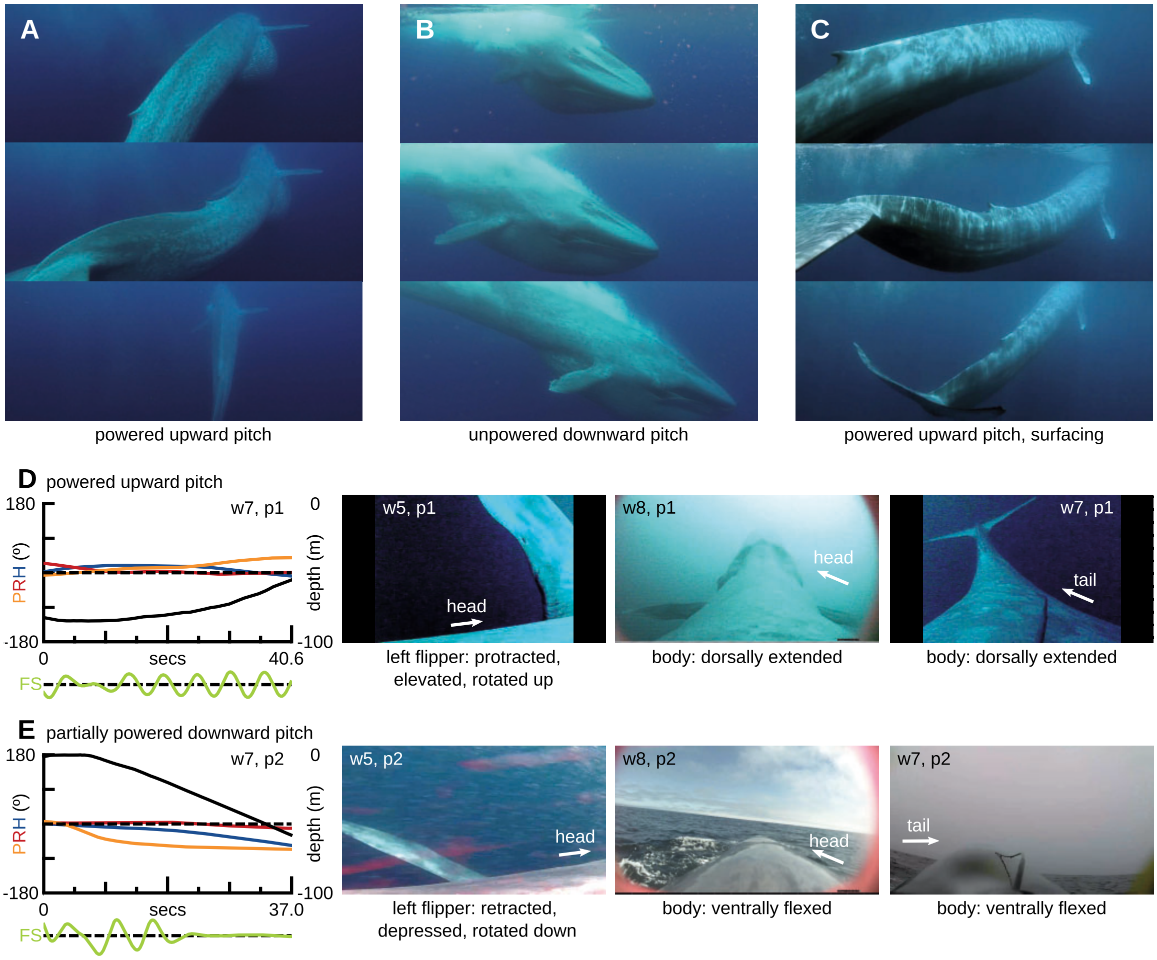

Fig. 2 Blue whales use their dorsoventral flexibility to perform pitch changes. **A**) A blue whale performs an upward pitching maneuver using dorsal extension and elevated flippers. **B**) A blue whale using ventral flexion and negative buoyancy to perform a downward pitch change while filtering. **C**) A whale uses dorsal flexion and depressed flippers to perform an upward pitch change while approaching the surface. **D**) Graphs and images from different whales demonstrate that upward pitch changes are performed with protracted, elevated, and upward rotated flippers, and dorsal extension. The individual whale (w) and maneuver number (p) are indicated in the panels and each panel is shown in context in the Supplementary Materials. The graph shows changes in pitch (P), roll (R), heading (H) of the body, the depth (black), and the nondimensional component of the pitch signal attributed to the fluking motion (FS). All images are shown at the instant of the maximum pitch change and images from the same individuals can be compared to determine the orientation of the control surfaces. **E**) Downward pitch changes are performed with retracted, depressed, downward rotated flippers, and a ventrally flexed body.

flipper rotates downward generating negative lift (Fig. 3D, E). This force asymmetry generates a rolling moment about the longitudinal axis of the body. The longer the hydrodynamic forces are applied, the greater the roll angle and the faster the rolling velocity (Fig. 1A). However, after prey engulfment when the buccal cavity is fully inflated the whale dramatically changes its mass, shape, and moment of inertia (Shadwick et al. 2013; Goldbogen 2018), and therefore the speed of filtering rolls is lower than that of maneuvering rolls (Fig. 1A, C). The 181 rolls we measured fit well with the relationship between roll angle and roll velocity predicted by a simple hydrodynamic model (Fig. 1A, Supplementary Material; Segre et al. 2016). Often at the midpoint of the roll, the flippers move from an elevated to depressed orientation, likely a result of the inertia of the body, and then are returned to an elevated position at the end of the roll (Fig. 1B, E, F). Although we have limited data on the role the flukes play in roll performance, it appears that the roll is initiated in the anterior part of the body using the flippers, while the posterior part of the body has a slight lag in roll orientation, suggesting that the flukes do not play an active role in roll execution.

Blue whales perform turns by rolling inward and dorsally extending their back, and thus turning velocity is correlated with roll angle (turn velocity =

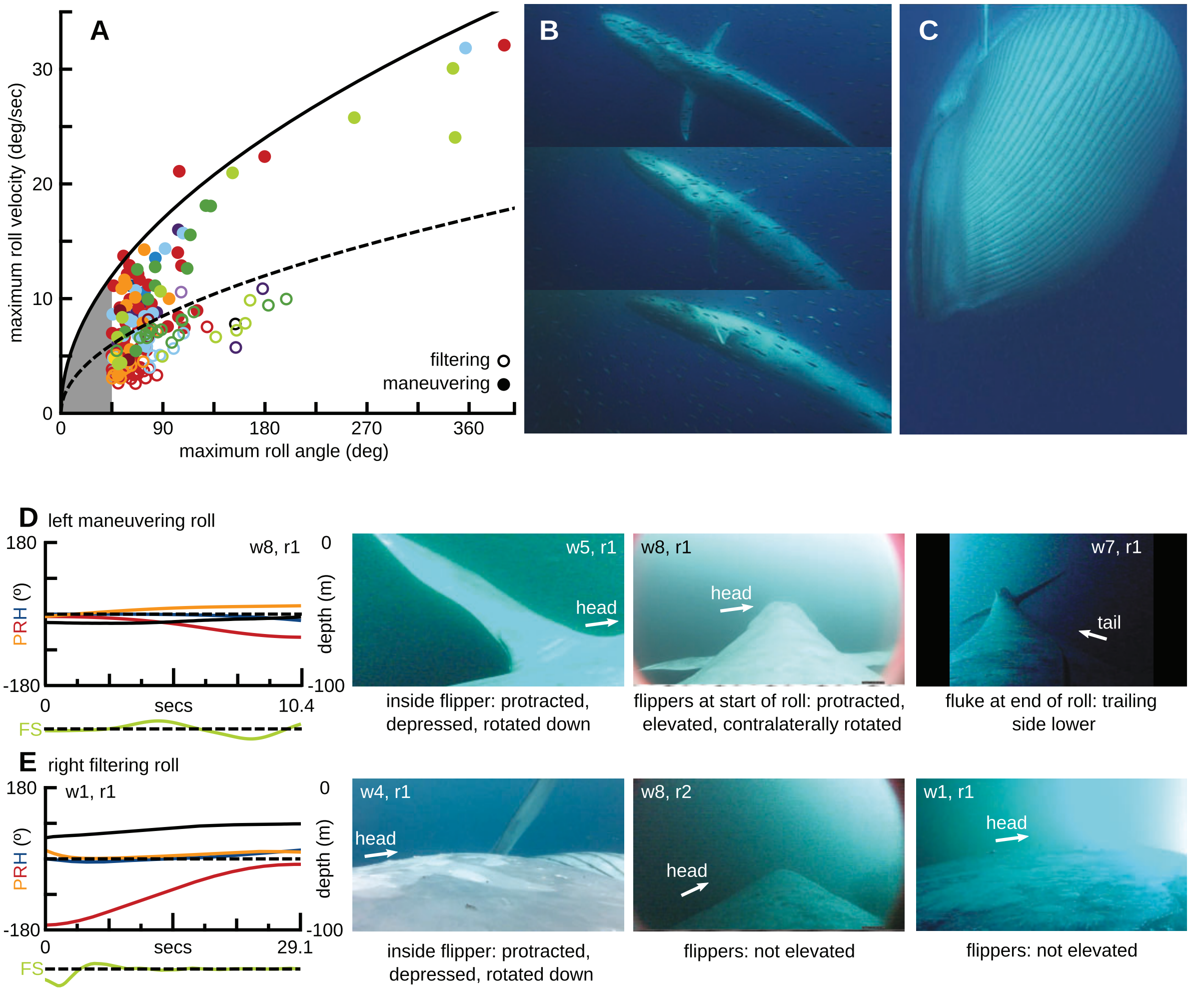

Fig. 3 Blue whales use contra-lateral flipper rotation to perform rolls. **A**) Rolling performance is predicted with a simple hydrodynamic model: rolls of longer duration attain higher angular velocity. Maneuvering rolls (solid) fit the curve predicted by an average rotational acceleration of 1.6°/s^2 while filtering rolls (open) fit the curve predicted by an average rotational acceleration of 0.4°/s^2 (derivations in the Supplementary Material). 181 rolls of >45° from 12 individual whales (different colors) are shown. **B**) A blue whale begins the roll with elevated, protracted, and contra-laterally rotated flippers which depress and protract during the middle of the roll and then extend again at the end. **C**) A filtering roll is performed with elevated, protracted flippers that may be constrained by the inflated pouch. **D**) Graphs and images from different whales demonstrate the orientations of the flippers during the course of the roll. The lower trailing edge of the fluke suggests that the flukes are not used to apply torque but rather follow the torsion of the body. The individual whale (w) and maneuver number (r) are indicated in the panels and each panel is shown in context in the Supplementary Materials. The graph shows changes in pitch (P), roll (R), heading (H) of the body, the depth (black), and the nondimensional component of the pitch signal attributed to the fluking motion (FS). Images are shown at the instant of the maximum roll velocity except when otherwise indicated and images from the same individuals can be compared to determine the orientation of the control surfaces. **E**) Filtering rolls are similar to maneuvering rolls except the whale's moment of inertia is larger, the translational speeds are slower, and the flippers are constrained by the inflated pouch, resulting in slower angular velocities.

0.13 * roll; $P < 0.001$; Fig. 4A, B, D and Fig 5F). However, blue whales also have the ability to perform turns while maintaining an upright posture and using lateral flexion (Fig. 4C, E and 5E). These types of level turns are low performance and often used while the whale is at the surface so that the blowhole can stay upright and out of the water. Inward banked turns begin with the flippers in an elevated and protracted position and with the outside flipper rotated up and the inside flipper rotated down (Fig. 4B, D). As the roll progresses the whale dorsally extents its back and rotates its inside flipper upward effectively performing a pitch-up maneuver while rolled on its side (Fig. 4B, D). Level turns can be performed either with the flippers in an elevated and protracted or with the flippers in a depressed position, which commonly occurs at the surface in order to keep the flippers submerged (Fig. 4C, E).

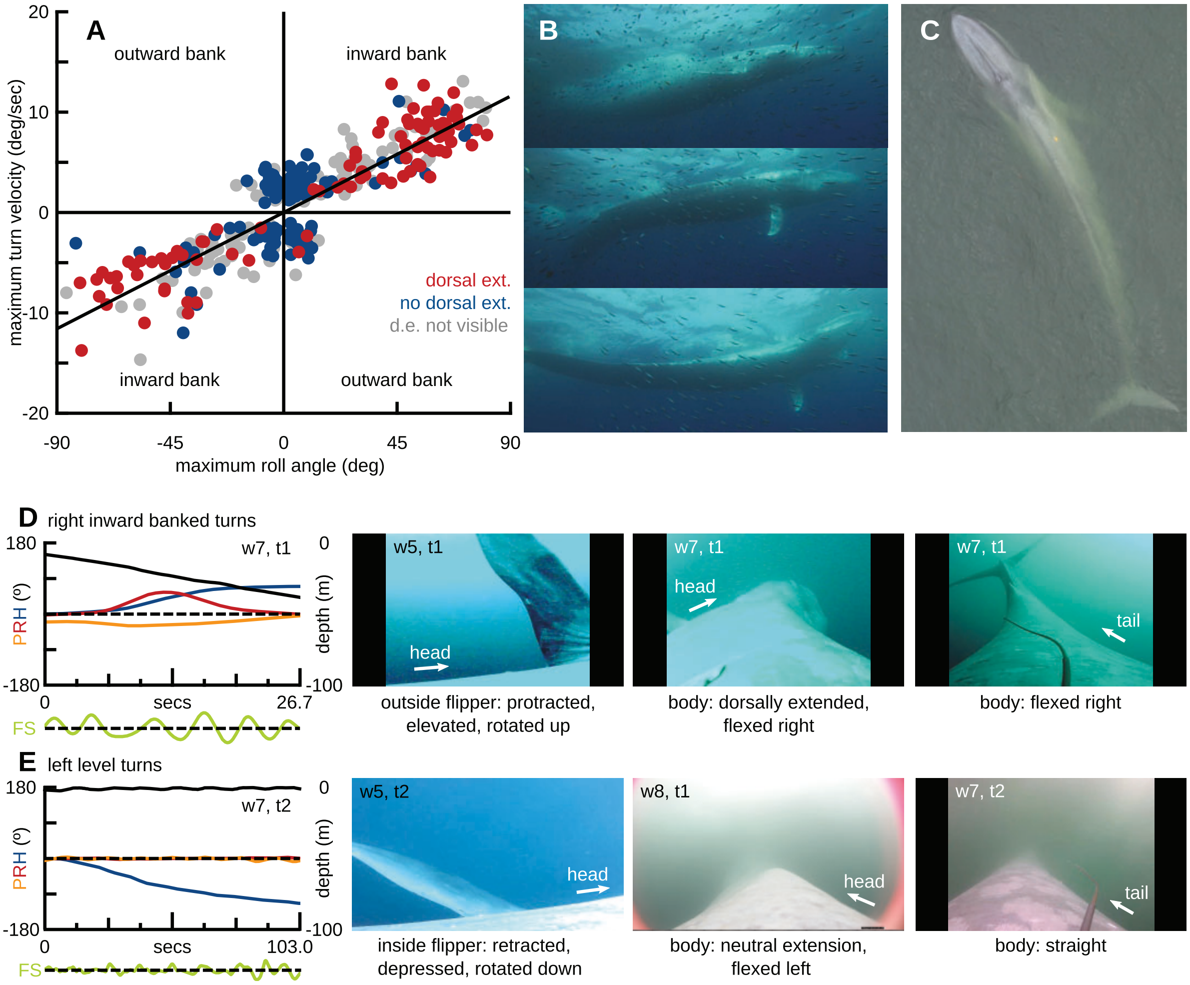

Fig. 4 Blue whales perform fast turns by banking inward. **A**) Turn velocity and bank angle are shown for 356 turns from 16 individual whales, indicated by different colors. Turn velocity is correlated with inward bank angle ($y = 0.13 * x$; $P < 0.001$). **B**) A blue whale uses protracted, elevated flippers, and dorsal extension to perform an inward banked turn while lunging. **C**) A blue whale uses its lateral body flexion to perform a level turn while keeping its flippers retracted, depressed, and underwater. **D**) Graphs and images from different whales demonstrate the orientations of the flippers and the flexion of the body during the course of the turn. The individual whale (w) and maneuver number (t) are indicated in the panels and each panel is shown in context in the Supplementary Materials. The graph shows changes in pitch (P), roll (R), heading (H) of the body, the depth (black), and the nondimensional component of the pitch signal attributed to the fluking motion (FS). Images are shown at the instant of the maximum turning velocity and images from the same individuals can be compared to determine the orientation of the control surfaces. **E**) Graphs and images from level turns performed at the surface while breathing.

Constructing complex maneuvers

To construct complex trajectories blue whales string together sequences of simple maneuvers. A common complex behavior is the “upward rolling lunge” (Fig. 6), where the whale approaches a prey patch from below, assumes a near vertical pitch angle, rolls its body to watch its prey, opens its mouth while pitching upward onto its back, and then rolls back to an upright position while filtering (Goldbogen et al. 2012; Friedlaender et al. 2017). In its simplest form the upward rolling lunge is sequentially composed of a pitch-up, a maneuvering roll, a second pitch-up during the lunge, and a filtering roll, and the movement of the flippers, flukes, and the body is similar to the movements used to perform the pure versions of these maneuvers. However, in many instances of the upward rolling maneuver, the pitching and rolling segments overlap temporally and often include heading changes. In the example presented in Fig. 6B, the upward roll begins while the whale is still pitching from horizontal to vertical. Likewise, after the lunge, the whale begins to roll back to an upright position while it is still performing the upside down pitch-up to horizontal.

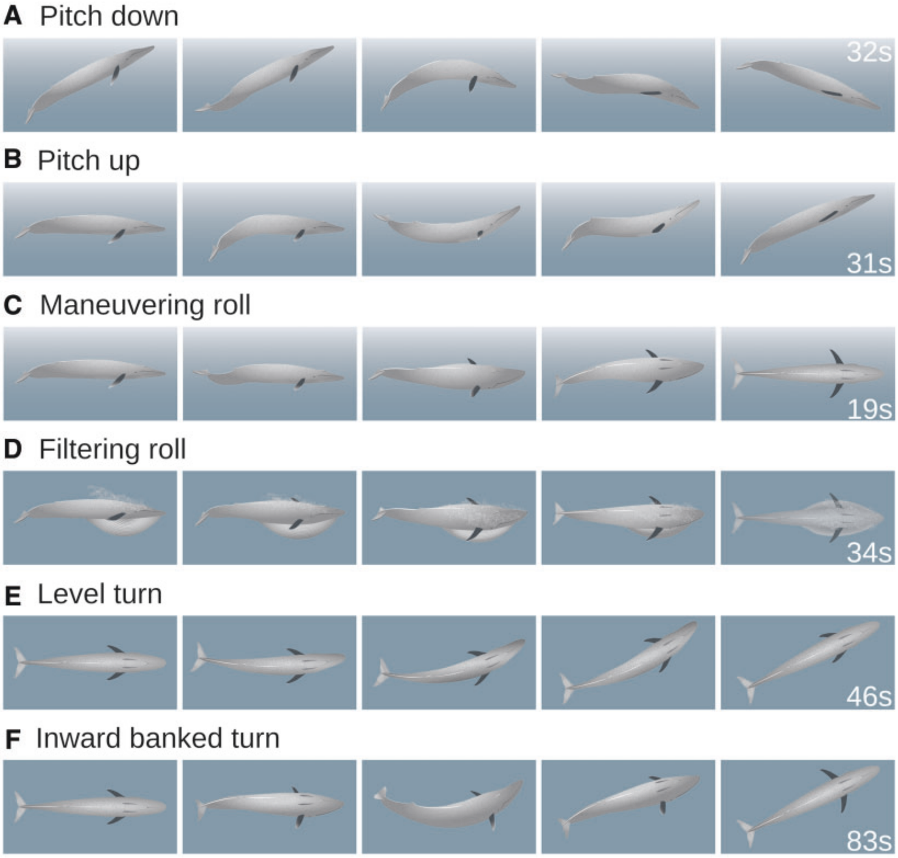

Fig. 5 A blue whale performs **A**) a downward pitch change by ventrally flexing its body and rotating its flippers downward. The flippers are not in an extended position. **B**) An upward pitch change by dorsally extending its body, extending its flippers, and rotating them upward. **C**) A maneuvering roll by extending its flippers and rotating them contra-laterally. The flukes twist, following the body. **D**) A filtering roll by extending its flippers and rotating them contra-laterally. The motion of the flippers may be constrained by the inflated buccal pouch. **E**) A level turn by laterally flexing its body while maintaining an upright roll. The flippers are not extended. **F**) An inward banked turn by rolling into the turn with extended flippers and then flexing its body dorsally, before rolling back to level. Illustration by Sylvia Heredia.

Powered versus unpowered maneuvering performance

Blue whales have the ability to perform both powered and unpowered maneuvers. However, most of the maneuvers we observed featured continuous fluke strokes or were partially powered, with periods of gliding interspersed with periods of fluking. Fish (1997, 2002) showed that when dolphins perform unpowered turns they uncouple the propulsive functions from the control functions of the flukes. This allows them to take advantage of increased spinal flexibility to perform higher angular velocity turns with lower radii. We did not find a similar pattern with blue whales: powered and unpowered turn velocities were not significantly different. This may be due to the fact that the fastest blue whale turns were highly banked and the whales were flexed dorsoventral instead of laterally. We did find that powered pitch-up, pitch-down, and maneuvering rolls were faster than their unpowered counterparts, although there was no difference between powered and unpowered filtering rolls. By powering through maneuvers, blue whales generate faster flow over the flippers. In turn this creates higher lift that can be used to change direction faster during a pitch or roll. These patterns may also be explained by the fact that many of the underpowered maneuvers performed by blue whales were still performed at speed, as the whale used its negative buoyancy to accelerate downward (Goldbogen et al. 2011; Goldbogen 2018).

Comparisons to other animals

As the largest animal in the world, blue whales are expected to have diminished maneuvering performance compared to smaller swimming organisms (Webb and De Buffrénil 1990; Domenici 2001). However, we have shown that in spite of their

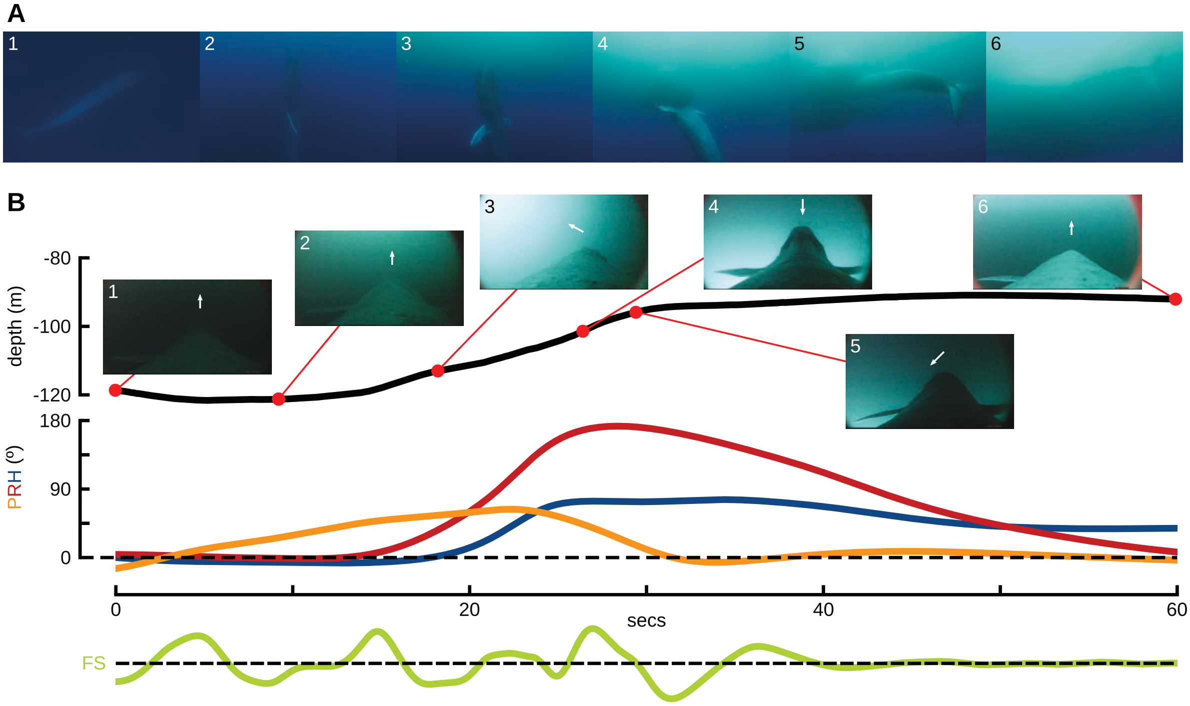

Fig. 6 Sequences of simple maneuvers are put together to navigate complex trajectories. **A**) A common complex behavior is the "upward rolling lunge," where the whale (1) approaches a prey patch from below, (2) assumes a near vertical pitch, (3) rolls to align itself with the prey, (4) opens its mouth while (5) pitching upward onto its back, (6) and then rolls back to an upright position while filtering. **B**) The depth profile (black), pitch (P), roll (R), heading (H), and nondimensional component of the pitch signal attributed to the fluking motion (FS). The photographs show how 1) the flippers are protracted and elevated as the whale is preparing for the maneuver; 2) the whale begins a pitch upward maneuver with flippers protracted and elevated and the body dorsally extended; 3) the whale performs a roll to the right with the right flipper protracted and elevated; 4) the whale opens its mouth performing an upside down pitch-up maneuver with flippers protracted, elevated, and symmetrically rotated up, and the body dorsally extended. 5) The whale, now upside down and horizontal, begins a partially powered filtering roll to the left with the flippers elevated and protracted and asymmetrically rotated so that the inside flipper is down and the outside flipper is up. 6) The whale is now horizontal and rolled upright. The arrows show the approximate direction of the surface based on the shadows in the images.

large body size, they still exhibit a remarkable degree of agility as they navigate their environment and hunt their prey (Goldbogen et al. 2012; Friedlaender et al. 2017). Like many other cetaceans, blue whales use the spinal flexibility that drives their fluke strokes (Long et al. 1997) to facilitate many of their maneuvers (Fish 1999, 2002), and this enhances their maneuvering performance when compared with similarly sized rigid-hulled vessels (Parson et al. 2011; Fish et al. 2018). Unsurprisingly, blue whale turning velocities are much slower than those of smaller cetaceans (Fish 2002). Unlike most odontocetes (toothed whales, dolphins, and porpoises), blue whales take advantage of their dorsal flexibility to perform turns by banking inwards. Many toothed whales perform turns by primarily flexing laterally and employing a slight inward bank (Fish and Rohr 1999; Fish 2002), but in contrast, blue whales bank up to 90° inward to perform fast turns and their turning speed is strongly correlated with bank angle. Little is known about how other species of baleen whale perform turns; however, there is some evidence that they use similar banking maneuvers (Edel and Winn 1978; Fish 1999). Blue whales clearly use their flippers to perform pitch changes and turns; however, it appears that many of these maneuvers can also be executed without the use of the flippers, at the cost of performance. As with other cetaceans, blue whales use their flippers to perform rolls (fin whales: Segre et al. 2016; spinner dolphins: Fish et al. 2006), but from our few videos with posteriorly-facing cameras we have no evidence to suggest that the whales supplement long-axis torque generated by the flippers with torque generated by the flukes. Enhanced maneuverability stemming from body flexibility and reconfiguration has been demonstrated in many other swimming animals including sharks (Porter et al. 2009, 2011), sea lions (Fish et al. 2003a), and manta rays (Fish et al. 2018), and this study shows that even at extremely large scales body flexibility can influence agility.

Table 1 Performance and kinematic characteristics of blue whale maneuvers

Maneuver	n	Angular vel (*M*±SD)	# powered	Timing of characteristics	Kinematic characteristics	#/visible
Pitch down	359	5.8°/s±1.6*	343	Mid	Flippers elevated and protracted	14/173
				Mid	Flippers rotated down	37/39
				Mid	Body extended dorsally	4/282
Pitch up	56	5.0°/s±1.3*	49	Mid	Flippers elevated and protracted	19/20
				Mid	Flippers rotated up	20/20
				Mid	Body extended dorsally	21/23
Maneuvering roll	110	9.4°/s±3.0**	89	Start	Flippers elevated and protracted	46/49
				Start to Mid	Flippers rotated contra-laterally	53/53
				Start to Mid	Fluke rotation trails roll direction	4/4
Filtering roll	71	6.9°/s±2.1**	23	Start	Flippers elevated and protracted	32/35
				Start to Mid	Flippers rotated contra-laterally	26/27
Level turn	143	2.7°/s±0.8***	131	Mid	Flippers elevated and protracted	8/73
				Mid	Body extended dorsally	3/111
				Mid	Body flexed laterally	29/43
				–	At water surface	120/143
Inward banked turn	205	5.8°/s±2.3***	178	Mid	Flippers elevated and protracted	101/115
				Mid	Body extended dorsally	88/121
				Mid	Body flexed laterally	46/79
				–	At water surface	3/205

Notes: The number of maneuvers that were powered (# powered), the timing of the kinematic characteristics (start/middle of maneuver), and the number of observations are presented (#/visible). Because of the camera placement, not all kinematic features were visible for every recorded maneuver. *, **, and ***denote significant difference between paired maneuvers.

A new control surface paradigm?

Due to their gigantic size, blue whales remain an important model organism for investigating the limitations of performance and scaling in the natural world. Taken together, our results illustrate the critical role that body flexibility plays in enhancing control and performance of maneuvers, even in the largest of animals. By flexing and extending their bodies the whales can reorient their flukes to produce off-axis forces and thus affect rotational maneuvers. We have strong evidence that this mechanism contributes to the performance of turns and pitch changes, since both of these maneuvers can be performed with the flippers in less prominent and less stereotyped positions. However, body flexibility may also play another role in enhancing maneuverability: enabling the use of secondary control surfaces such as the peduncle, the head, and the palate in generating steering forces. The use of non-hydrofoil body parts for hydrodynamic maneuvering performance has been documented in other swimming and flying animals. For example, flap-bounding birds manipulate their body angles to control lift and drag (Tobalske 2010), electric rays use their body to generate lift while gliding (Rosenblum et al. 2011), flying snakes shape their body to form hydrofoils used for gliding and steering (Socha et al. 2005), and ants falling out of trees use their head to maneuver in the horizontal plane (Yanoviak et al. 2010). Likewise in large whales, the body and peduncle may serve as a rudder (Fish 2002), the head may contribute to pitch control, and the palate may produce a torque that facilitates flow entry into the buccal cavity during lunge feeding (Cooper et al. 2008). These body parts are not shaped like airfoils and although they may not generate much hydrodynamic lift, they may create enough asymmetric drag to produce torque during particular maneuvers. Increased reliance on these secondary control surfaces to supplement torques produced by the flukes and flippers may also provide a way for these massive animals to increase their maneuvering performance beyond standard isometric predictions. Testing these predictions will require detailed hydrodynamic models of the body and the control surfaces, a three-dimensional understanding of maneuvering kinematics, and a comparative analysis of performance across rorqual species. Our study offers the first analysis of the breadth of maneuvers performed by blue whales, along with an attempt to qualify the role that the flippers, flukes, and body flexibility play in executing and maintaining the maneuvers. As technological innovations in remote tracking improve a more detailed hydrodynamic analysis of free-swimming blue whale locomotion will be possible, and this will undoubtedly allow for a better understanding of their ecology, energetics, and hydrodynamic design.

Acknowledgments

We thank the captain and crew of the RV John Martin and the RV Truth for logistical support and the teams from Cascadia Research Collective and Moss Landing Marine Laboratory for assistance in the field. Aerial photographs were provided by the Duke Marine Robotics and Remote Sensing Lab. Underwater videos, reproduced here with permission, were filmed for the BBC television series "The Hunt" by Hugh Pearson, copyright Silverback Films/David Reichert, in collaboration with J. Calambokidis. All procedures were conducted under approval of the National Marine Fisheries Service (permits 16111, 19116, 15271); National Marine Sanctuaries (MULTI-2017-007); and institutional IACUC committees.

Funding

This research was funded in part by grants from the National Science Foundation (IOS-1656676), the Office of Naval Research (N000141612477), and a Terman Fellowship from Stanford University.

Supplementary data

Supplementary data available at *ICB* online.

References

Aoki K, Amano M, Mori K, Kourogi A, Kubodera T, Miyazaki N. 2012. Active hunting by deep-diving sperm whales: 3D dive profiles and maneuvers during bursts of speed. Mar Ecol Prog Ser 444:289–301.

Cade DE, Barr KR, Calambokidis J, Friedlaender AS, Goldbogen JA. 2018. Determining forward speed from accelerometer jiggle in aquatic environments. J Exp Biol 221:jeb.170449.

Cade DE, Friedlaender AS, Calambokidis J, Goldbogen JA. 2016. Kinematic diversity in rorqual whale feeding mechanisms. Curr Biol 26:2617–24.

Cooper LN, Sedano N, Johansson S, May B, Brown JD, Holliday CM, Kot BW, Fish FE. 2008. Hydrodynamic performance of the minke whale (*Balaenoptera acutorostrata*) flipper. J Exp Biol 211:1859–67.

Domenici P. 2001. The scaling of locomotor performance in predator–prey encounters: from fish to killer whales. Comp Biochem Physiol Part A Mol Integr Physiol 131:169–82.

Edel RK, Winn HE. 1978. Observations on underwater locomotion and flipper movement of the humpback whale Megaptera novaeangliae. Mar Biol 48:279–87.

Fish FE. 1996. Transitions from drag-based to lift-based propulsion in mammalian swimming. Am Zool 36:628–41.

Fish FE. 1997. Biological designs for enhanced maneuverability: analysis of marine mammal performance. Tenth International Symposium on Unmanned Untethered Submersible Technology Special Session on Bio-Engineering Research Related to Autonomous Underwater Vehicle. Durham, NH: Autonomous Undersea Systems Institute. p. 109–17.

Fish FE. 1999. Performance constraints on the maneuverability of flexible and rigid biological systems. Proceedings of the Eleventh International Symposium on Unmanned Untethered Submersible Technology. Durham, NH: Autonomous Undersea Systems Institute. p. 394–406.

Fish FE. 2002. Balancing requirements for stability and maneuverability in cetaceans. Integr Comp Biol 42:85–93.

Fish FE. 2004. Structure and mechanics of nonpiscine control surfaces. J Ocean Eng 29:605–21.

Fish FE, Battle JM. 1995. Hydrodynamic design of the humpback whale flipper. J Morphol 225:51–60.

Fish FE, Hurley J, Costa DP. 2003a. Maneuverability by the sea lion *Zalophus californianus*: turning performance of an unstable body design. J Exp Biol 206:667–74.

Fish FE, Kolpas A, Crossett A, Dudas MA, Moored KW, Bart-Smith H. 2018. Kinematics of swimming of the manta ray: three-dimensional analysis of open-water maneuverability. J Exp Biol 221:jeb166041.

Fish FE, Lauder GV. 2017. Control surfaces of aquatic vertebrates: active and passive design and function. J Exp Biol 220:4351–63.

Fish FE, Nicastro AJ, Weihs D. 2006. Dynamics of the aerial maneuvers of spinner dolphins. J Exp Biol 209:590–8.

Fish FE, Peacock JE, Rohr JJ. 2003b. Stabilization mechanism in swimming odontocete cetaceans by phased movements. Mar Mammal Sci 19:515–28.

Fish FE, Rohr JJ. 1999. Review of dolphin hydrodynamics and swimming performance. Technical report.

Fish FE, Weber PW, Murray MM, Howle LE. 2011. The tubercles on humpback whales' flippers: application of bio-inspired technology. Integr Comp Biol 51:203–13.

Friedlaender AS, Herbert-Read JE, Hazen EL, Cade DE, Calambokidis J, Southall BL, Stimpert AK, Goldbogen JA. 2017. Context-dependent lateralized feeding strategies in blue whales. Curr Biol 27:R1206–8.

Goldbogen JA. 2018. Physiological constraints on marine mammal body size. Proc Natl Acad Sci U S A 115:3995–7.

Goldbogen JA, Cade DE, Boersma AT, Calambokidis J, Kahane-Rapport SR, Segre PS, Stimpert AK, Friedlaender AS. 2017. Using digital tags with integrated video and inertial sensors to study moving morphology and associated function in large aquatic vertebrates. Anat Rec 300:1935–41.

Goldbogen JA, Calambokidis J, Friedlaender AS, Francis J, DeRuiter SL, Stimpert AK, Falcone E, Southall BL. 2012. Underwater acrobatics by the world's largest predator: 360°

rolling manoeuvres by lunge-feeding blue whales. Biol Lett 9:20120986.

Goldbogen JA, Calambokidis J, Oleson E, Potvin J, Pyenson ND, Schorr G, Shadwick RE. 2011. Mechanics, hydrodynamics and energetics of blue whale lunge feeding: efficiency dependence on krill density. J Exp Biol 214:131–46.

Johnson MP, Tyack PL. 2003. A digital acoustic recording tag for measuring the response of wild marine mammals to sound. IEEE J Ocean Eng 28:3–12.

Long JH, Pabst DA, Shepherd WR, McLellan WA. 1997. Locomotor design of dolphin vertebral columns: bending mechanics and morphology of *Delphinus delphis*. J Exp Biol 200:65–81.

Parson JM, Fish FE, Nicastro AJ. 2011. Turning performance of batoids: limitations of a rigid body. J Exp Mar Bio Ecol 402:12–8.

Porter ME, Roque CM, Long JH. 2009. Turning maneuvers in sharks: predicting body curvature from axial morphology. J Morphol 270:954–65.

Porter ME, Roque CM, Long JH. 2011. Swimming fundamentals: turning performance of leopard sharks (*Triakis semifasciata*) is predicted by body shape and postural reconfiguration. Zoology 114:348–59.

Rosenblum HG, Long JH, Porter ME. 2011. Sink and swim: kinematic evidence for lifting-body mechanisms in negatively buoyant electric rays *Narcine brasiliensis*. J Exp Biol 214:2935–48.

Sato K, Watanuki Y, Takahashi A, Miller PJ, Tanaka H, Kawabe R, Ponganis PJ, Handrich Y, Akamatsu T, Watanabe Y, et al. 2007. Stroke frequency, but not swimming speed, is related to body size in free-ranging seabirds, pinnipeds and cetaceans. Proc R Soc B Biol Sci 274:471–7.

Segre PS, Cade DE, Fish FE, Potvin J, Allen AN, Calambokidis J, Friedlaender AS, Goldbogen JA. 2016. Hydrodynamic properties of fin whale flippers predict maximum rolling performance. J Exp Biol 219:3315–20.

Segre PS, Seakamela SM, Meÿer MA, Findlay KP, Goldbogen JA. 2017. A hydrodynamically active flipper-stroke in humpback whales. Curr Biol 27:R636–7.

Sfakiotakis M, Lane DM, Davies JBC. 1999. Review of fish swimming modes for aquatic locomotion. IEEE J Ocean Eng 24:237–52.

Shadwick RE, Goldbogen JA, Potvin J, Pyenson ND, Vogl AW. 2013. Novel muscle and connective tissue design enables high extensibility and controls engulfment volume in lunge-feeding rorqual whales. J Exp Biol 216:2691–701.

Simon M, Johnson M, Tyack P, Madsen PT. 2009. Behaviour and kinematics of continuous ram filtration in bowhead whales (*Balaena mysticetus*). Proc R Soc B Biol Sci 276:3819–28.

Socha JJ, O'Dempsey T, LaBarbera M. 2005. A 3-D kinematic analysis of gliding in a flying snake, *Chrysopelea paradisi*. J Exp Biol 208:1817–33.

Tobalske BW. 2010. Hovering and intermittent flight in birds. Bioinspir Biomim 5:45004.

Webb PW. 1988. Simple physical principles and vertebrate aquatic locomotion. Integr Comp Biol 28:709–25.

Webb PW. 2004. Maneuverability—general issues. IEEE J Ocean Eng 29:547–55.

Webb PW, De Buffrénil V. 1990. Locomotion in the biology of large aquatic vertebrates. Trans Am Fish Soc 119:629–41.

Weber PW, Howle LE, Murray MM, Reidenberg JS, Fish FE. 2014. Hydrodynamic performance of the flippers of large-bodied cetaceans in relation to locomotor ecology. Mar Mammal Sci 30:413–32.

Weihs D. 1993. Stability of aquatic animal locomotion. Contemp Math 141:443–61.

Williams TM. 1999. The evolution of cost efficient swimming in marine mammals: limits to energetic optimization. Philos Trans R Soc Lond Ser B Biol Sci 354:193–201.

Williams TM. 2006. Phisiological and ecological consequences of extreme body size in whales. In: Estes JA, DeMaster DP, Doak DF, Williams TM, Brownell RL Jr, editors. Whales, whaling and ocean ecosystems. Berkeley (CA): University of California Press. p. 191–201.

Woodward BL. 2006. Locomotory strategies, dive dynamics, and functional morphology of the mysticetes: Using morphometric, osteology, and DTAG data to compare swim performance in four species of baleen whales. Ph.D. Orono, ME: Dissertation, University of Maine.

Yanoviak SP, Munk Y, Kaspari M, Dudley R. 2010. Aerial manoeuvrability in wingless gliding ants (*Cephalotes atratus*). Proc R Soc B Biol Sci 277:2199–204.